CHAPTER 2.

An Illuminating Framework:

Understanding the Photoluminescence of α-$CuAlCl_4$

Roger M. Sullivan and James D. Martin*

Department of Chemistry, North Carolina State University, Raleigh, NC 27695-8204.

(As Published in *Journal of the American Chemical Society*; **1999**; *121*, 10092-10097.)

Abstract

$CuAlCl_4$ exemplifies a new class of phosphors based on metal halide analogs of aluminophosphates. The α- and β-$CuAlCl_4$ phases show brilliant blue to blue-green luminescence. The electronic structure of the $CuAlCl_4$ corner sharing tetrahedral frameworks has been explored by fluorimetric and diffuse reflectance measurements on the isomorphous series α-$CuAlBr_xCl_{4-x}$ (x=0-4). The photoluminescence is demonstrated to be a bulk property of the electronically isolated $CuCl_{4/2}$ tetrahedra within the framework matrix. Remarkably, the structural framework is flexible such that at least one mole of small molecule gasses per $CuAlCl_4$ formula unit can be reversibly sorbed. The sorption/desorption of small molecule gasses further results in the reversible quenching of the photoluminescence.

2.1 Introduction

We recently described the use of $CuCl_{4/2}$ and $AlCl_{4/2}$ tetrahedral building units for the construction of open framework solids.[1,2] Like silicates, the assembly of corner sharing tetrahedral metal halide units can be exploited for the synthesis of a variety of framework materials. In the metal-halide system, $ZnCl_2$ can be envisioned as a silicate type parent phase. (Note that α-$ZnCl_2$ is isostructural to the high cristoballite phase of SiO_2.)[3] Substituting certain of the Zn(II) sites with Cu(I) results in the formation of anionic frameworks, $[Cu_nZn_{m-n}Cl_{2m}]^{n-}$, analogous to zeolitic aluminosilicates.[4] Similarly, structural analogues to aluminophosphates, $Al_mP_mO_{4m}$, can be synthesized utilizing Cu(I) and Al(III) to yield $Cu_mAl_mCl_{4m}$ frameworks. Two such materials, α- and β-$CuAlCl_4$, represent condensed-phase framework materials derived from closest packed anion sublattices.[2]

An apparent flexibility of this framework allows for the remarkable chemisorption of small molecule gases. The reversible binding of small molecules such as CO, C_2H_4 and C_6H_6, to $CuAlCl_4$ in solution has previously elicited significant interest for both separations and catalysis applications.[5] During our investigation of the chemisorption into crystalline α- and β-$CuAlCl_4$, we observed an room temperature blue luminescence under both UV and X-ray excitation. The photoluminescence described here provides a useful probe of the interaction between the framework and sorbed gases since the sorption of small molecules quenches the blue luminescence. Heavy atom

substitution to form the isomorphous α-$CuAlBr_4$ and α-$CuGaCl_4$ structures[2] also quenches the room temperature luminescence.

A diverse range of materials in which copper (I) serves as the luminescent activator exhibit emissions across the visible spectrum. When doped into silicate glasses[6] or zinc chalcogenide phosphors[7] a blue to green luminescence is observed, whereas a red to orange emission is observed for $Cu_4I_4L_4$ clusters (L=alkylamine).[8] Similarly, models used to describe Cu(I) luminescence vary widely.[9] Molecular orbital models are frequently used to describe copper (I) doped alkali or alkaline metal halides,[10] ion-exchanged zeolites,[11] and other oxides[12] in which cuprous ions reside in well-characterized coordination environments. By contrast, in zinc chalcogenides, copper (I) is described as an extrinsic defect in an electronic band model.[13] Emissions originating from copper (I) cluster excited states are reported both for molecular tetramers and clustered defects in extended solids such as $SrCl_2:Cu^+$.[14] In both halide and heavier chalcogenides, significant mixing of the ligand *p* and metal *d* orbitals has led some to emphasize the halide-to-metal charge transfer (XMCT) character of the $3d^{10} \rightarrow 3d^9 4s$ absorption.[15] Species with low lying π^* ligand orbitals, such as $Cu_4I_4py_4$, exhibit emissions arising from metal-to-ligand charge transfer (MLCT) excited states.[16] The unique structure of copper aluminum chloride, in which the d^{10} copper centers are isolated within a tetrachloroaluminate matrix, provides an excellent host to study the luminescence of Cu(I). Furthermore, the ability to form a chloride/bromide solid solution affords the opportunity to examine the role of the anion in the luminescence mechanism. Luminescence of the metastable β-phase, and samples of the α-phase prepared by rapid

thermal quenching of the melt, appear to have an additional contribution from a red shifted defect site Cu(I) activator. While both α- and β-$CuAlCl_4$ exhibit brilliant room temperature photoluminescence, this manuscript focuses on the luminescent mechanism for copper (I) on the unique crystallographic site of the α-phase unit cell.

2.2 Results

Excitation /Emission. The excitation and emission spectra for α- and β-$CuAlCl_4$ are plotted in Figure 2.1. The brilliant blue emission of the α-phase, (solid line) at 20.5 x 10^3 cm^{-1} (483 nm), is also readily observed upon illumination with a hand held mercury lamp (254 nm excitation) under daylight conditions. The ratio of incident to emissive intensity is approximately 2/3 that of a $CaWO_4$ standard. Similar emission is observed upon excitation with X-rays. (The emission at room temperature due to X-ray excitation is brilliant when using synchrotron radiation (16 MeV, 1 Å) and more faint when using radiation from a sealed copper tube.) The emission maximum is slightly red shifted for β-$CuAlCl_4$, (dashed line) at 19.8 x 10^3 cm^{-1} (505 nm). Excitation maxima for both the α-phase (solid line) and β-phase (dashed line) are observed at 37.0 x 10^3 cm^{-1} (275 nm). As previously reported, the β-phase is metastable with respect to the α-phase; and is prepared by rapid cooling of the molten salt in ice water.[2] Samples of α-$CuAlCl_4$ prepared from a rapid thermal quench of the melt also show this red shift in the emission maximum under 254 nm excitation. The energy shifts between the excitation and emission maxima (16.1 x 10^3 cm^{-1} for α-$CuAlCl_4$ and 17.2 x 10^3 $cm^{-1}$for β-$CuAlCl_4$) are notably large.

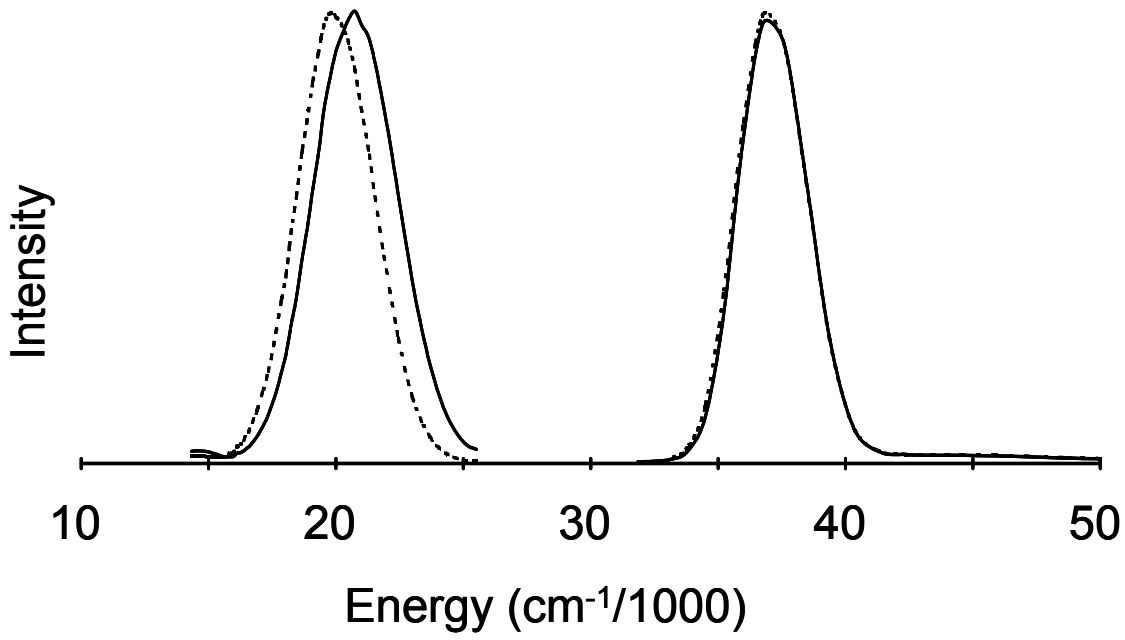

Figure 2.1. The excitation and emission spectra of α-$CuAlCl_4$ (solid line) and β-$CuAlCl_4$ (dashed line).

Diffuse Reflectance. The diffuse reflectance data for α-$CuAlCl_4$ is plotted as the remission spectrum in Figure 2.2.a. Remission spectra may be interpreted in the same manner as absorption spectra.[17] This spectrum is described by two broad absorption features centered around 40.3 x 10^3 cm^{-1} [248 nm] and 49.8 x 10^3 cm^{-1} [201 nm]. Addition of bromine to form the $CuAlBr_xCl_{4-x}$ solid solution has no significant influence on the onset of absorption (i.e., the band edge falls at 35.4 (± 0.5) x 10^3 cm^{-1} [282 (± 3) nm] for all α-$CuAlBr_xCl_{4-x}$ (x=0-4)), as shown in Figure 2.2. The resolution of two maxima upon increasing bromide substitution suggests that in the all chloride spectrum the dominant low energy feature is the sum of multiple features. By contrast the same anion substitution causes the higher energy features to broaden and dramatically increase in intensity.

Luminescence of the mixed halide solid solution. Substitution of either the chloride anions with bromide ions or the aluminum cations with gallium cations results in the quenching of the room temperature luminescence. In a liquid nitrogen bath both α-$CuAlBr_4$ and α-$CuGaCl_4$ luminesce blue under 254 nm excitation. Taking advantage of this room temperature quenching of the luminescence upon anion substitution, we examined the series of mixed chloride-bromide phases, α-$CuAlBr_xCl_{4-x}$ (x = 0-4). A non-linear decrease in the luminescent intensity with increasing the bromide content, x, was observed (Figure 2.3), in contrast to the Vegard's Law linear dependence of the unit cell volume on the bromide substitution (Figure 2.4).[18]

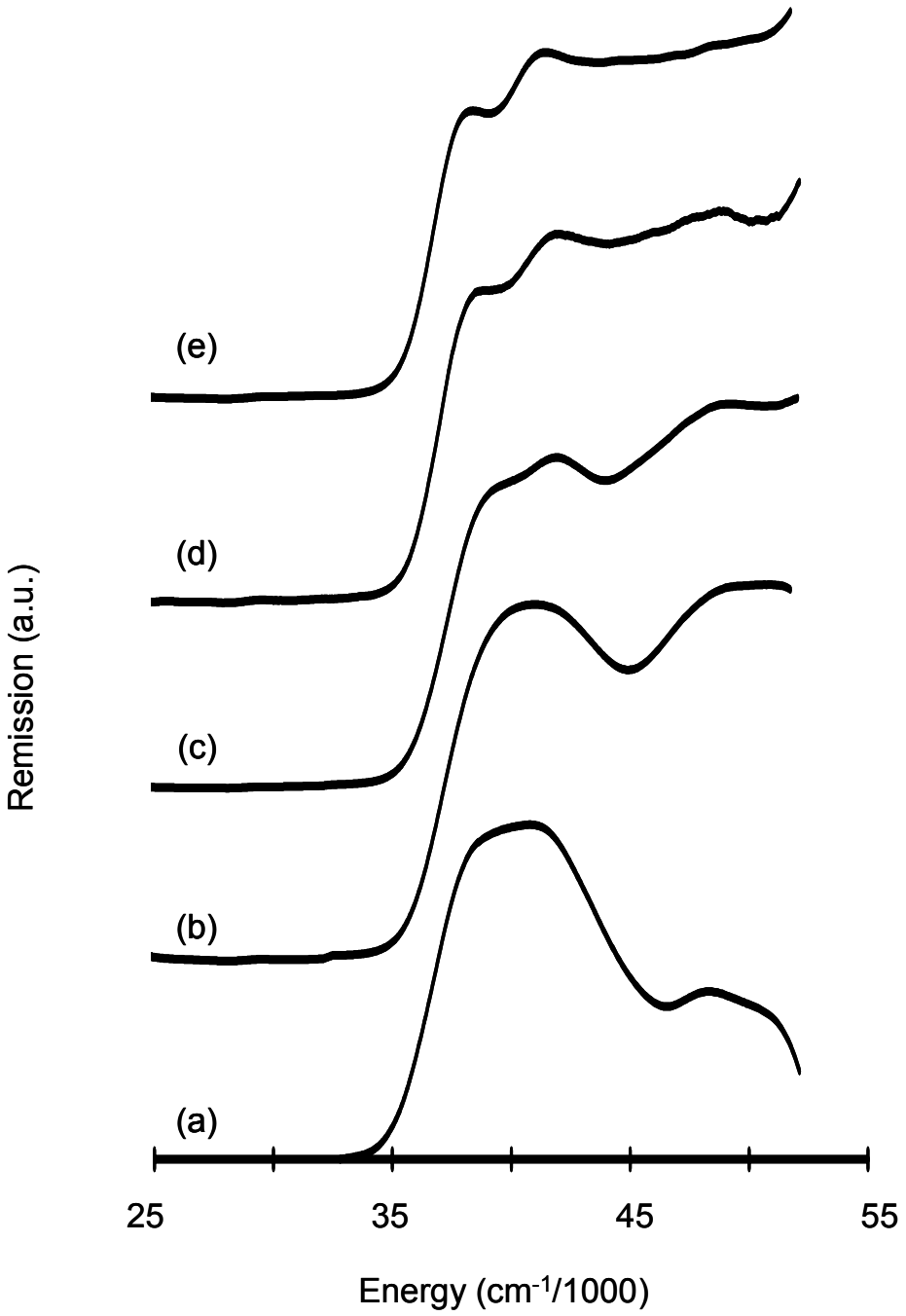

Figure 2.2. Reflectance data for the series $CuAlBr_xCl_{4-x}$, plotted as the remission function, $F(R\infty) = (1-R\infty)^2/2R\infty$ (based on the Kubelka-Munk theory of diffuse reflectance):[17] (a) $CuAlCl_4$, (b) $CuAlBrCl_3$, (c) $CuAlBr_2Cl_2$, (d) $CuAlBr_3Cl$, and (e) $CuAlBr_4$.

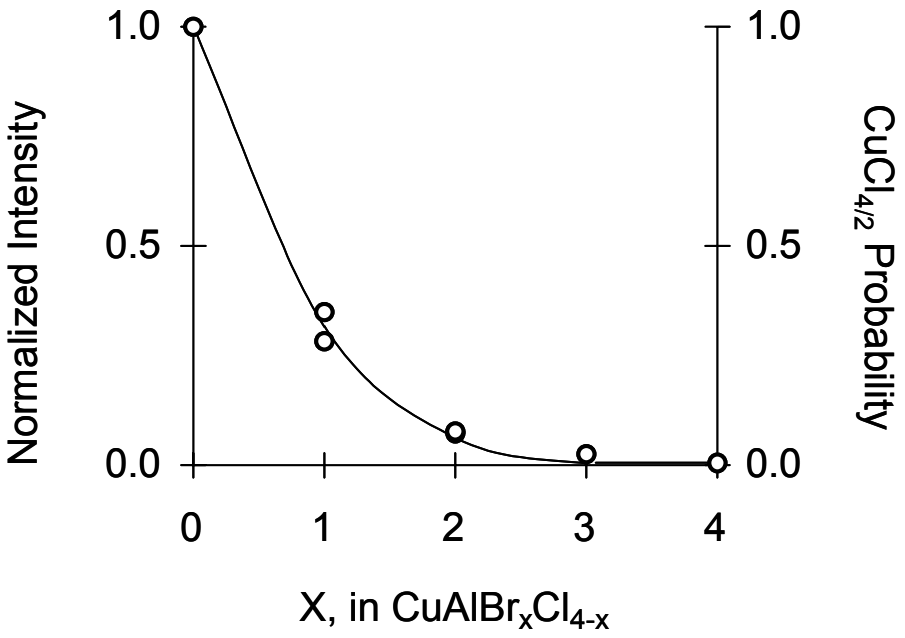

Figure 2.3. The normalized emission intensity of the solid solutions α-$CuAlBr_xCl_{4-x}$, x = 0-4 (plotted as solid circles). The solid line is a plot of the probability of the four halide sites around each copper cation being occupied by only chloride anions ($[(4 - x)/4]^4$).

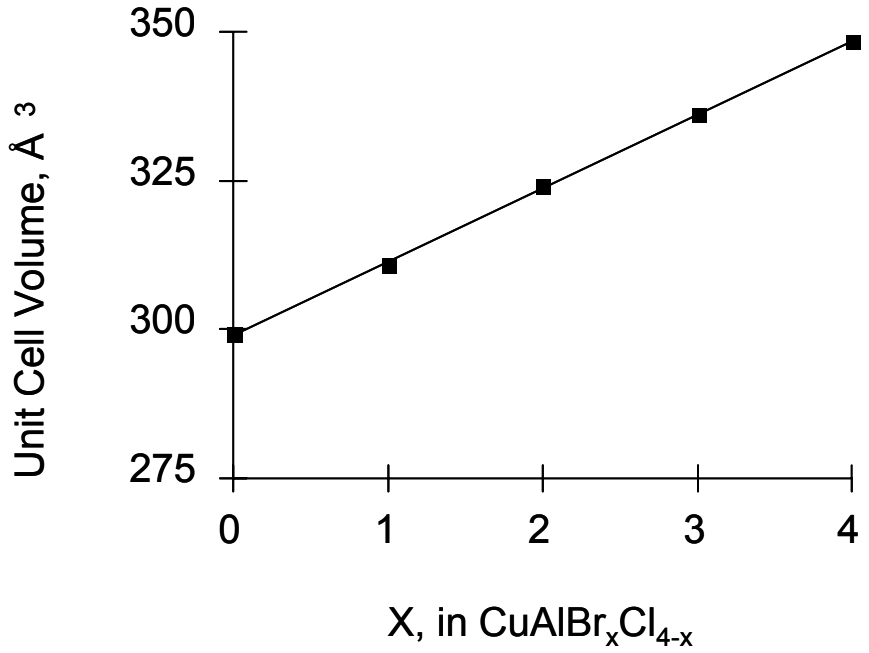

Figure 2.4. Plot of the unit cell volume as a function of the solid solutions α-$CuAlBr_xCl_{4-x}$, x = 0-4 (plotted as solid circles).

Luminescence Lifetime. The luminescent lifetime of α-$CuAlCl_4$ was determined by frequency domain fluorometery.[19] The modulation and phase curves extracted from the time dependent intensity data fit a model with a 95% contribution by a single exponential decay, τ=14.2 μsec ($\chi^2 = 2.6$). The remaining 5% of the signal is attributed to scattered light from a grating artifact at twice the excitation wavelength.

Luminescence Quenching by Gas Sorption. $CuAlCl_4$ can repeatedly and reversibly sorb and desorb, at least one equivalent per framework formula unit of certain small molecule gases (such as ethylene, carbon monoxide and benzene vapor).[20] Data for the room temperature equilibrium volumetric measurements for the sorption of ethylene (shown in Figure 2.5) exhibits a type-V isotherm, which is reminiscent of a cooperative binding of the gas to the framework.[21] Upon gas sorption there is a marked change to the framework structure[22] that further results in the quenching of all photoluminescence. The sorbed gas is readily removed under dynamic vacuum resulting in a return of the luminescence as seen in Figure 2.6.

2.3 Discussion

Reflectance and Luminescence. The structures of α-$CuAlCl_4$ and its binary precursors, CuCl and $AlCl_3$, are related but the ternary chloride exhibits remarkable luminescence not seen in the binary precursors. Aluminum trichloride displays a cubic closest packed (ccp) chloride sublattice in which aluminum cations occupy octahedral interstices. Both CuCl and α-$CuAlCl_4$ also display a cubic closest packing (ccp) of the

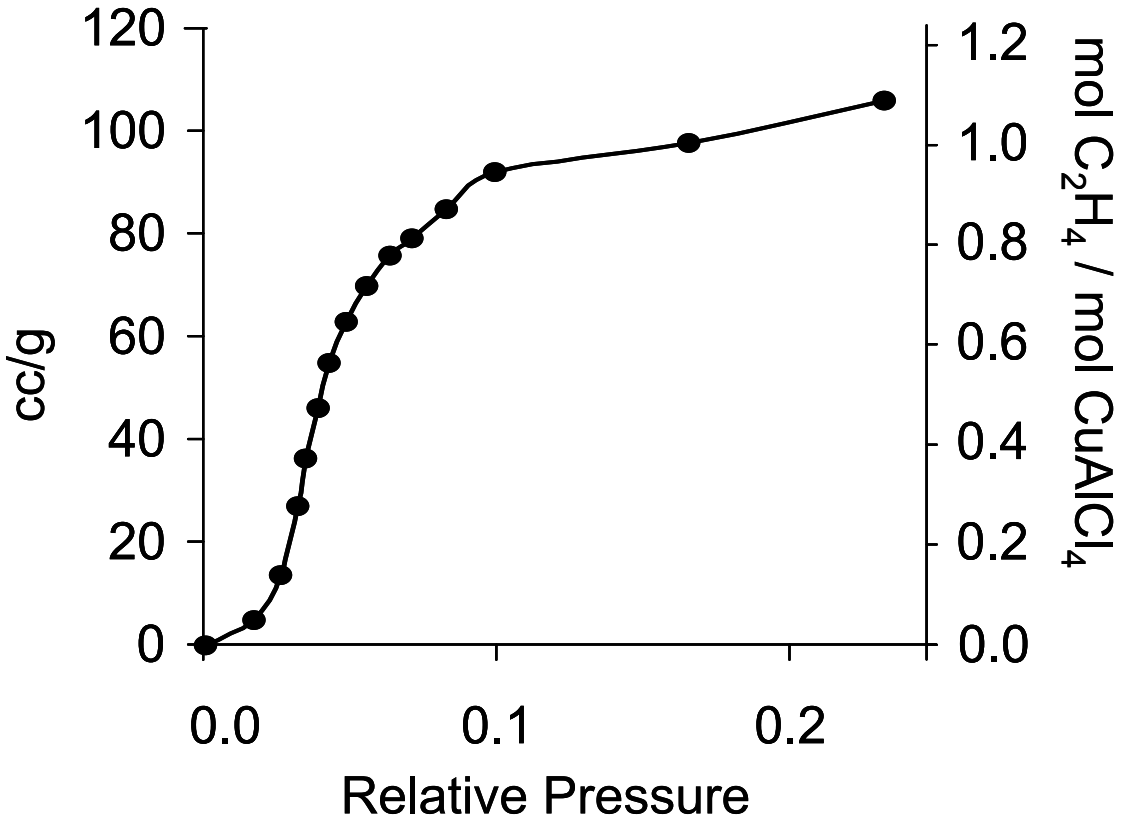

Figure 2.5. Chemisorption plotted as a function of relative pressure for the sorption of ethylene into α-$CuAlCl_4$.

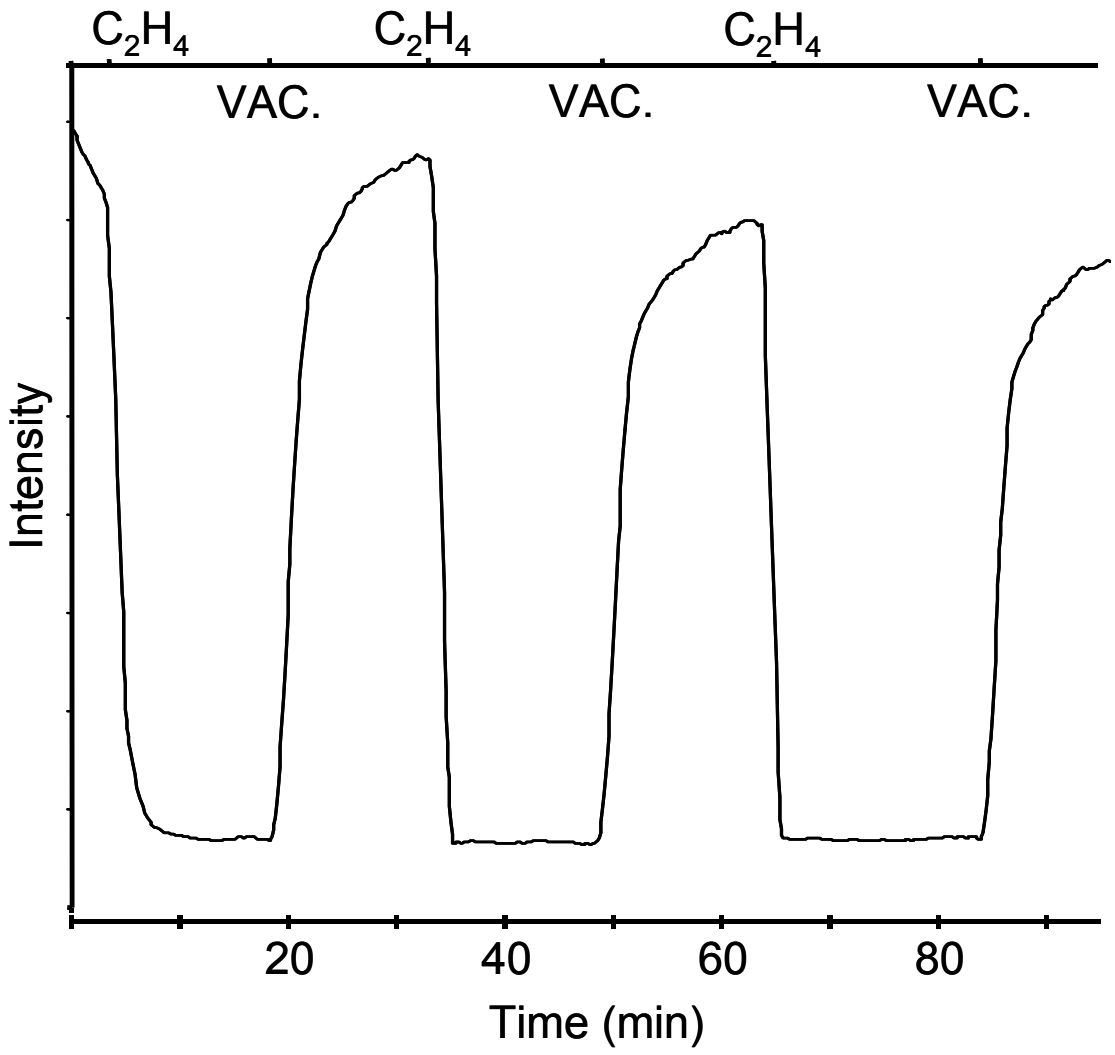

Figure 2.6. Emission intensity (monitored at $\lambda = 483$ nm) plotted as a function of the reversible sorption of ethylene into α-$CuAlCl_4$.

chloride anions, but with all cations distributed among corner sharing tetrahedral interstices.[23,24] No light is absorbed by $AlCl_3$ at energies accessible to our instrumentation (below 52.6 x 10^3 cm^{-1} [190 nm, 6.5 eV]). The contribution of aluminum orbitals to α-$CuAlX_4$ is expected to be only at high energy; and thus they participate only in the high-energy features of the diffuse reflection spectra. Extended Huckel calculations[25] indicate that both α-$CuAlCl_4$ and CuCl exhibit a direct band gap in which the valence band is a mixture of Cl 3*p* and Cu 3*d* orbitals and the orbital character of the conduction band edge is dominated by the Cu 4*s* contribution. The low energy edge of the diffuse reflectance spectrum in Figure 2.2.a yields an estimated band gap for α-$CuAlCl_4$, of 34.9 x 10^3 cm^{-1} [287nm, 4.3 eV].[26] The band gap of this ternary halide is much higher in energy than the 25.8 x 10^3 cm^{-1} [388 nm, 3.2 eV] reported for CuCl.[27] This disparity in band gaps is consistent with a localized versus delocalized electronic structure for $CuAlCl_4$ and CuCl, respectively. In the structure of α-$CuAlCl_4$ the $CuCl_{4/2}$ tetrahedral units are completely separated from each other by corner sharing $AlCl_{4/2}$ tetrahedra such that the nearest copper-copper contacts are 5.43 Å. In the binary chloride the $CuCl_{4/2}$ tetrahedra are also corner sharing, but each tetrahedron is linked to four other $CuCl_{4/2}$ tetrahedra with copper-copper separations of 3.74 Å.

To further understand the relationship between structure and optical properties we prepared the isomorphous series α-$CuAlBr_xCl_{4-x}$ (x = 0-4). The series forms a true solid solution, displaying a Vegard's Law linear dependence of unit cell volume on bromide substitution (Figure 2.4) and no superstructure in the powder X-ray diffraction. The diffuse reflectance spectra for the series α-$CuAlBr_xCl_{4-x}$ are displayed in Figure 2.2.

Because the higher energy absorption centered around 47 × 10^3 cm^{-1} broadens and increases in intensity upon increasing bromide substitution, we have assigned this absorption to halide-to-metal charge transfer (XMCT). An increased participation of the bromide 4*p* orbitals is expected since they are higher in energy than the chloride 3*p*. The low energy feature centered about 40 x 10^3 cm^{-1} in the α-$CuAlCl_4$ spectra (Figure 2.2.a) resolves into multiple peaks on increasing bromide substitution. In contrast to the absorption edge of the respective binary halides (CuCl = 24.9 × 10^3 cm^{-1} and CuBr = 23.0 × 10^3 cm^{-1}), the low energy features do not substantially shift in energy. Comparing the diffuse reflectance spectra in Figure 2.2, it is observed that the onset of absorption for the series α-$CuAlBr_xCl_{4-x}$ falls at nearly the same value, 35.4 ± 0.3 x 10^{-3} cm^{-1} (268 ± 3 nm). The independence of the remission band edge from halide substitution supports the assignment to a copper centered $3d^{10} \rightarrow 3d^9 4s$ absorption.

The excitation maximum for the blue luminescence in $CuAlCl_4$, 37.0 x 10^3 cm^{-1} (275 nm), falls in the region of the absorption edge and thus is assigned to a Cu $3d^{10} \rightarrow 3d^9 4s$ transition. While the excitation energy of the luminescence remains essentially the same for all values of the Br/Cl solid solution, the intensity of the blue emission dies out with increasing bromide substitution as shown in Figure 2.3. Remarkably, the nonlinear loss of emission intensity can be fit to an equation that describes the probability of any copper cation being surrounded by four chlorides. By assuming that in the solid solution all chlorides and bromides are randomly distributed among the halide crystallographic sites, the probability that any copper is surrounded by four chlorides is equal to the probability of any one site being occupied by a chloride,

raised to the fourth power, $[(4-x)/4]^4$. The super position of this probability curve onto the normalized emission intensity (Figure 2.3) demonstrates that the emission intensity is directly proportional to the decrease in the number of all chloride ($CuCl_{4/2}$) centers upon bromide substitution. The quenching of luminescence by substitution with a heavy element, such as bromine, is well known. Typically the increased spin-orbit coupling by the heavy element relaxes the $\Delta S=0$ selection rule such that a non-radiative pathway from a triplet excited state to the singlet ground state is favored. Emission from a triplet state of α-$CuAlCl_4$ is confirmed by the measured lifetime of 14.2 μsec. The lifetime data is best fit to a single exponential, indicating that the observed blue luminescence arises from a single emissive center. We conclude from this that the activator for the blue luminescence is the copper tetrachloride tetrahedral building block, $CuCl_{4/2}$ and that the luminescence is a bulk property of α-$CuAlCl_4$. We suspect that the red shifting of the emission maximum observed for the β-phase (Figure 2.1), prepared by rapid cooling from the melt, and α-phase samples with a similar history of rapid cooling, is a result of an increased defect population. A defect structure in which interstitial coppers or coppers on aluminum sites form clustered copper defects could result in such a decreased energy gap. The sum of less intense, red shifted, defect cluster emission and the dominant blue emission of the isolated copper (I) centers could red shift the observed emission maximum.

It is useful to treat the optical properties of this extended solid in terms of a localized molecular orbital model; similar to the case of calcium tungstate. A localized molecular orbital model of an isolated, d^0, WO_4^{2-} tetrahedron has been very useful for

explaining its optical properties.[28] By extension, we utilize an isolated, d^{10}, $CuCl_4^{3-}$ tetrahedron to interpret the optical properties of α-$CuAlCl_4$. The copper (I) cations reside on a crystallographic position with S_4 site symmetry, which exhibits a slight compression of the $CuCl_{4/2}$ tetrahedra along the S_4 axis. The allowed transitions for a $CuCl_4^{3-}$ fragment of S_4 symmetry are described in Figure 2.7. The set of three allowed $3d^{10} \rightarrow 3d^9 4s$ transitions and two $3d^{10} \rightarrow 3d^9 4p$ transitions, as well as some possible transitions from the chloride lone pairs into the copper 4*s*, gives rise to the absorption feature centered at 40.3 x 10^3 cm^{-1} [248 nm, 5 eV] (Figure 2.2.a). However, as noted above, the halide contribution is not sufficient to influence any significant variation in the energy of the transitions upon bromide for chloride substitution. The triplet-states derived from these orbitals are also given in Figure 2.7. While these triplet states do not correspond to allowed transitions from the singlet ground state, the emission lifetime of 14.2 μsec implies that a triplet state is involved in the emissive relaxation.

Based on the above assignments, the Jablonski diagram in Figure 2.8 provides a summary the observed optical behavior of the α-$CuAlCl_4$ system. Starting from the right, the diagram shows the ground state singlet and the three singlet excited states belonging to the $3d^{10} \rightarrow 3d^9 4s$ orbital transition. The lowest lying triplet-state, which represents a formally forbidden transition from the singlet manifold, is schematically shown at the left. The overlay of the emission, excitation and diffuse reflectance spectra (Figure 2.8.b) leads us to conclude that the maximum absorbance (**abs**) is into a high lying excited state of the singlet manifold. After rapid relaxation (**R**) to the vibrational

ground state of a high lying singlet excited state, the process of internal conversion (**IC**) allows for the

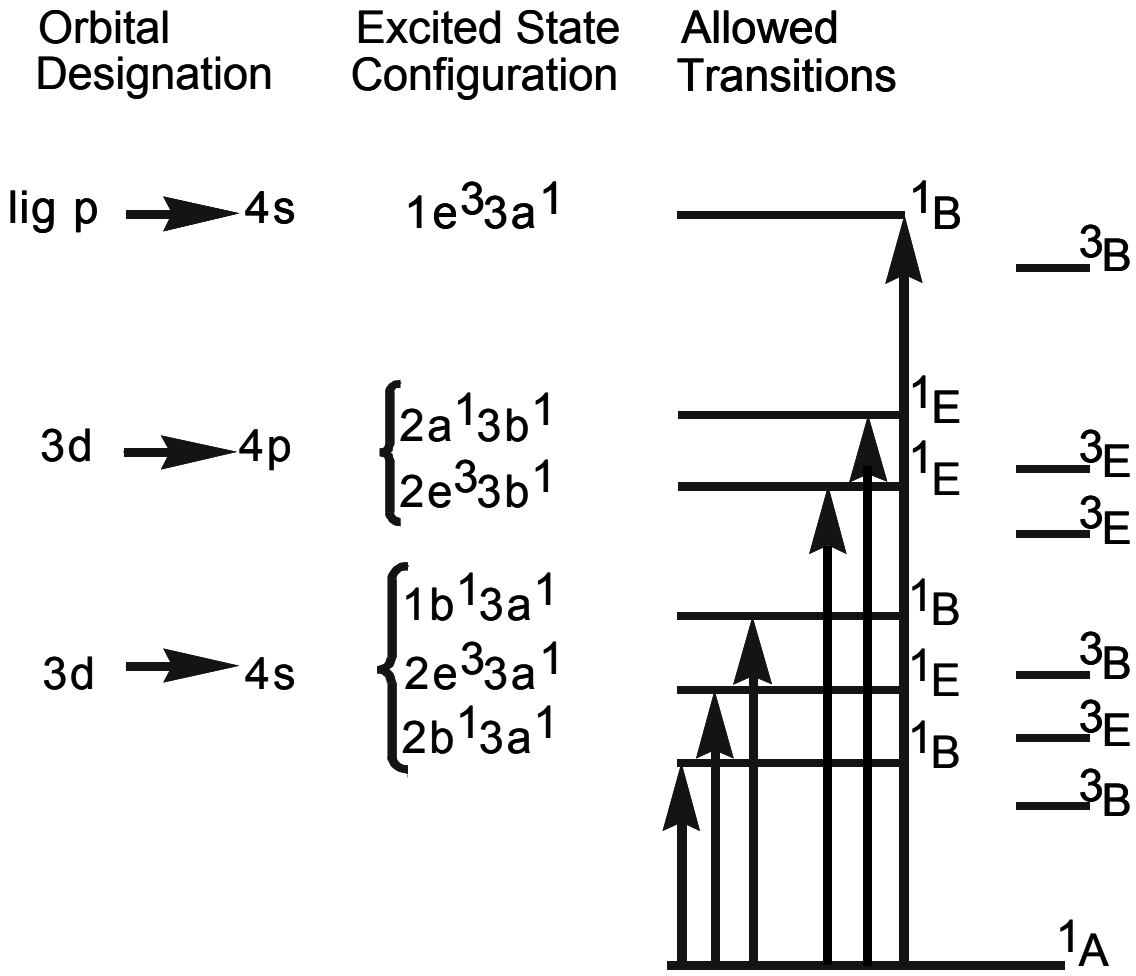

Figure 2.7. State diagram for $CuCl_4^{3-}$. The ordering of the excited state singlets are from the diffuse-reflectance spectrum.

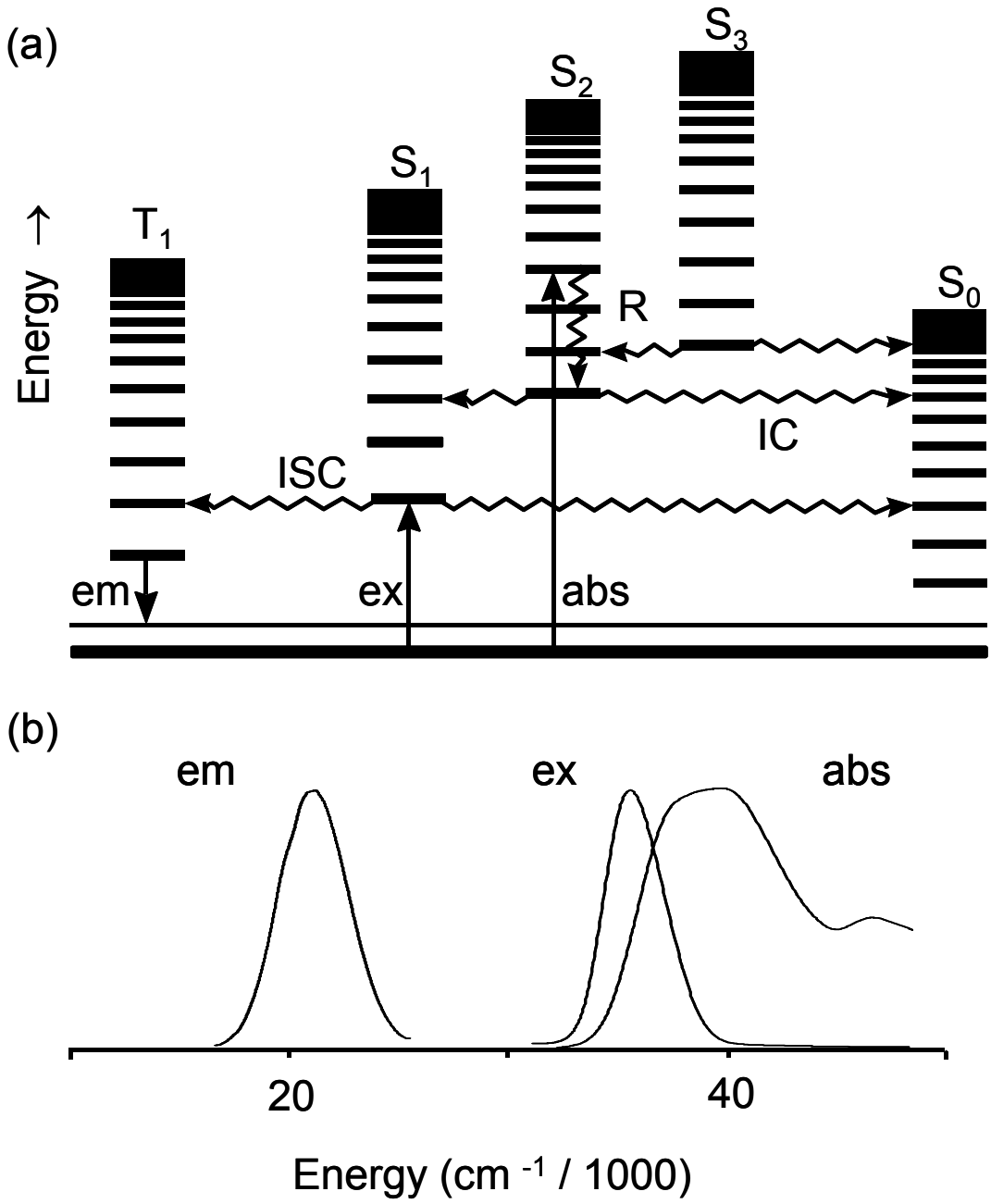

Figure 2.8. a) Jablonski diagram for $CuCl_4^{3-}$. Radiative processes, including emission (em), excitation (ex), and absorption (ab) are indicated by straight arrows. Non-radiative processes, including inter-system crossing (ISC), internal conversion (IC) and vibrational relaxation (R), are indicated by squiggled arrows. b) Observed spectra for α-$CuAlCl_4$.

non-radiative relaxation through the singlet manifold to the singlet ground state. However, absorbance at the excitation maximum (**ex**) is into the lowest lying singlet state (close to the absorption edge). Again rapid relaxation to the vibrational ground state of the lowest singlet excited state occurs, but now with few accessible energy overlaps on the excited state hypersurface leading to the singlet ground state, intersystem crossing (**ISC**) into the lowest lying triplet state becomes competitive with internal conversion. Once formed the lowest lying triplet state decays radiatively to a vibrationally excited singlet ground state (**em**). The singlet-triplet energy difference is equal to twice the exchange integral,[29] which is theoretically large in a highly localized system such as an isolated cation. The bulk of the 16.3×10^3 cm^{-1} energy shift between the excitation and emission maxima is thus associated with the spin forbidden transition from the singlet to triplet excited states.[30] In addition a smaller, but significant, contribution to the energy shift is expected from the vibronic coupling of the electronic transition with a Jahn-Teller type distortion of the $3d^9 4s$ excited state.[31] In addition to the excited-state Jahn-Teller type distortion, which compresses the tetrahedra along the S_4 axis, vibronic coupling with the totally symmetric stretch is expected, based on the strong anti-bonding nature of the copper 4*s* orbital. The full width at half maximum for the emission peak is ~4000 cm^{-1}. This is consistent with a large difference in the equilibrium nuclear configurations of the excited-state triplet and the singlet ground state.[9]

Luminescent Quenching by Gases. Variation in the room temperature luminescence, on exposure to small molecule gases, includes copper aluminum chloride in a group of inorganic materials which can act as a gas sorption sensors.[32, 33] A plot of gas sorbed by α-$CuAlCl_4$ at room temperature as a function of relative pressure, P_S/P_0, is

shown in Figure 2.5. After reaching the relative pressure for the onset of sorption, approximately 0.02 Torr, there is a rapid increase in the amount of gas sorbed up to about one equivalent of gas per formula unit. The shape of this curve is suggestive of a cooperative binding process where coordination of a few sorbant molecules alters the structure of the sorbate such that additional molecules sorb more readily.[34] Upon exposure of copper aluminum chloride to ethylene an abrupt drop in emission intensity is observed corresponding to the gas sorption (Figure 2.6). Upon exposure to dynamic vacuum (~.05 Torr) the sorbed gas is removed and the luminescence returns. These 10 minute gas on, 10 minute gas off cycles, shown in Figure 2.6, are repeated demonstrating the reversibility of the process. A major structural reorganization is required to accommodate the sorption of ethylene into the framework of α-$CuAlCl_4$, which we are currently studying by time resolved powder X-ray diffraction.[22] Precise structural details are not yet fully understood, however, the weak sorbant-sorbate interactions favor a non-radiative relaxation of the copper centered excited state.

2.4. Conclusion

The unique choice of building blocks for the three dimensional framework of α-$CuAlCl_4$ has led to its brilliant, room temperature, blue luminescence. The $CuCl_{4/2}$ corner-sharing tetrahedral building units are well isolated by $AlCl_{4/2}$ tetrahedra in the framework structure. These isolated copper (I) centers serve as intrinsic activators giving rise to a brilliant blue luminescence. The heavy ion substitution in the solid solution $CuAlBr_xCl_{4-x}$ results in the quenching of luminescence that is directly proportional to the

statistical distribution of Br throughout the lattice. The flexibility of the metal halide structure is responsible for the reversible binding of small molecules by α-$CuAlCl_4$. The coupling of photoluminescence and gas sorptive properties leads to a useful probe of the chemistry of the system.

2.5. Experimental

General Methods and Procedures. All reactions and products are air and moisture sensitive and were handled under the inert atmosphere of an N_2 filled glove box or using vacuum and Schlenk line techniques. Aluminum trichloride (Fluka) was purified by sublimation from an Al/NaCl flux.[35] Aluminum bromide was prepared by reaction of the elements[36] (Aldrich) and purified by sublimation from an Al/KBr flux. The cuprous halides were prepared by comproportionation of copper metal (EM Science) and $CuCl_2$ (Aldrich) or $CuBr_2$ (Matheson) dissolved in the appropriate mineral acid (HCl or HBr) and precipitated upon dilution with deoxygenated water.[37] The cuprous halides were then purified by sublimation. Gallium chloride was used as received from Aldrich. All powder X-ray diffraction measurements were obtained using an Enraf-Nonius Guinier camera and were indexed with respect to silicon as a standard.

Synthesis of α-$CuAlX_4$ (X=Cl, Br). As previously reported,[1] α-$CuAlCl_4$ (m.p. 236°C) is prepared from the melt of the respective binary halides. In order to prepare materials of the highest optical purity, it is important to heat the reaction mixture to near the melting point of the cuprous halide (430°C for CuCl and 504°C for CuBr), and, to

perform the reaction with a slight excess (1.0 wt%) of the aluminum trihalide. In a typical reaction, CuCl (4.250 g, 42.93 mmol) and $AlCl_3$ (5.781 g, 43.36 mmol) were placed into a fused silica tube and sealed under vacuum. The reaction vessel was then heated to 430°C for one hour and cooled to room temperature at a rate of 10°C/hr. The resulting product was characterized by powder X-ray diffraction and by diffuse reflectance spectroscopy. The mixed halide materials α-$CuAlBr_xCl_{4-x}$, as well as α-$CuGaCl_4$, were similarly prepared from stoicheometric melts of the binary components. There is no evidence for a superstructure by powder diffraction in the α-$CuAlBr_xCl_{4-x}$ phases and the mixed halides show a linear dependence of the unit cell volume on bromide substitution, x , (cell volume $= (12.35x/4 + 286.77)$ Å^3).

Spectroscopy. Diffuse reflectance measurements were carried out on a Cary 3e UV-Vis spectrophotometer equipped with an integrating sphere. Spectra were measured with respect to a pressed polytetrafluoroethylene powder standard. Reflectance spectra were collected as $R_\infty = R_{sample}/R_{refrence}$, then plotted as the remission function, $F(R_\infty)=(1-R_\infty)^2/2R_\infty$ (based on the Kubelka-Munk theory of diffuse reflectance).[17]

Steady state fluorescence spectra were measured with an ISS PC-1 fluorometer equipped with a Xenon arc lamp using a front face detection geometry to orient the sample face at an angle of 22.5° with respect to the incident beam. A low band pass UG-11 filter was placed after the excitation monochromater. Excitation spectra were corrected by a rhodamine-B quantum counter. Emission spectra were corrected with respect to a standard quinine sulfate solution and the NIST spectrum. Emission spectra were plotted using the relative emitted energy per constant interval ($\Phi_E = \Phi_\lambda \lambda^2/hc$).[38]

Emission intensity measurements were normalized using $CaWO_4$ as an external standard. Scattered light from a grating artifact at 346 nm was also found to be a valid internal standard for normalizing emission intensities.

Time resolved phosphorescence measurements were performed on an ISS K2-003 Fastscan Multi-frequency Phase and Modulation Fluorometer. Data were collected for ten frequencies in the range of 10 KHz to 70 KHz. Standard deviation for the measurements was 0.2° for the phase values and 0.004° for the modulation values.

Gas Sorption. Measurement of the luminescence upon gas sorption and desorption were carried out on samples prepared by coating 2 g of ground fused silca particles (300-800 microns) with 0.06 g α-$CuAlCl_4$ (mp 236° C) in a fused silica tube. The tube was heated to 250° C and cooled at a rate of 1 °C/min. The tube was then connected to a gas/vacuum manifold and the intensity at the emission maximum measured as a function of time, during which the sample was alternately evacuated and exposed to gas. Data for C_2H_4 are presented in this work, however other small molecule gasses including CO, NO and benzene have also been examined.[20] All gases were used as received from Aldrich of National Gas Products. Gunier powder X-ray diffraction films were obtained for samples of α-$CuAlCl_4$ in capillaries before gas sorption and were found to match the same samples after desorption. Gas adduct phases were also characterized by powder X-ray diffraction films.

Equilibrium volumetric measurements for the sorption of ethylene were made on modified Coulter SA3100 BET surface area analyzer. Samples of α-$CuAlCl_4$ (~30 mg) were placed in the sample chamber at room temperature. A free volume measurement

was performed using He gas before the sample was dosed with calibrated aliquots of ethylene. Using this system, it was possible to perform equilibrium measurements up to a pressure of approximately 200 torr.

Acknowledgements. The authors gratefully acknowledge Dr. Martin van de Ven of ISS Fluorescence Instrumentation for the frequency domain lifetime measurements, Michael Peachey for the volumetric gas sorption measurements and Coulter Corporation for the loan of the SA3100 BET surface area analyzer. This work was supported by the National Science Foundation, CAREER award (DMR-9501370). J. D. Martin is a Cottrell Scholar of the Research Cooperation.

2.6. References

1. Martin, J. D.; Dattelbaum, A. M.; Thornton, T. A.; Sullivan, R. M.; Yang, J.; Peachey, M. T. *Chem. Mat.* **1998**, 10, 2699.

2. Martin, J. D.; Leafblad, B. R.; Sullivan, R. M.; Boyle, P. *Inorg. Chem.* **1998**, *37*, 1341.

3. a) Brehler, B. *Naturwissenschaften* **1959**, 554. b) Barth, T. F. W. *Am. J. Sci.* **1932**, 350.

4. Martin, J. D.; Greenwood, K. B. *Angew. Chem., Int. Ed. Eng.* **1997**, 36, 2072.

5. (a) Walker, D. G. *Prepr. Am. Chem. Soc., Div. Pet. Chem.* **1983**, 28, 746. (b) Hirai, H; Nakamura, M.; Komiyama, M. *Bull. Chem. Soc. Jpn.* **1983**, 56, 2519. (c) Hirai, H.; Wada, K.; Komiyama, M. *Bull. Chem. Soc. Jpn.* **1986**, 59, 1043. (d) Hirai, H; Hara, S; Komiyama, M. *Bull. Chem. Soc. Jpn.* **1986**, 59, 1051.

6. Debnath, R.; Das, S. K. *Chem. Phys. Lett.* **1989**, 52.

7 Kroeger; Hellingman *Trans. Faraday Soc.* **1948**, 156.

8. Kyle, K.R.; Ryu, C. K.; DiBenedetto, J. A.; Ford, P.C. *J. Amer. Chem. Soc.*, **1991**, 113, 2954.

9. Blasse, G. *Adv. Inorg. Chem.*, **1990**, 35, 319.

10. (a) Chermette, H.; Pedrini, C. *J. Chem. Phys*., **1981**, 75, 1869. (b)Fussgaenger, K. *Phys. Stat. Sol.*, **1969**, 36, 645. (c) Baldin, G; Jean, A. ; Spinolo, G. *Phys. Stat. Sol.*, **1968**, 25, 557. (d) Patil, R. R.; Moharil, S. V. *J. Lum.* **1995**, 63, 339. (e) Patil, R. R.; Miharil, S. V. *J. Lum.* **1995**, 65, 321.

11. Texter, J.; Strome, D. H.; Herman, R. G.; Kller, K. *J. Phys. Chem*., **1977**, 81, 333.

12. Barrie, J. D.; Dunn, B.; Stafsudd, O. M.; Nelson, P. *J. Lum.* **1987**, 37, 303.

13. (a) Peka, P.; Schulz, H-J. *Sol. State Comm.* **1984**, 89(3), 225. (b) Bowers R.; Melamed N. T. *Phys. Rev.* **1955**, 99, 1781. (c) Van Gool, W. Thesis , University of Amsterdam, Netherlands, 1961.

14. (a) Yamashita, N.; Ebisumori, K.; Nakamura, K. *J. Lumin*., **1994**, 62, 303-311.(b) Payne, S. A.; McClure, D. S. *J. Phys. Chem*., **1984**, 88, 1379-1385.

15. Jørgensen K. Chemical Bonding Inferred from Visible and Ultraviolet Absorption Spectra. In *Solid State Physics; Advances in Research and Applications, Vol. 13*; Seitz, F.; Turnbull, D. Eds.; Academic, New York, 1962, p. 430.

16. Ford, P. C.; *Coord. Chem. Rev.* **1994**, 2196.

17. Wendlandt, W.W.; Hecht, H. G. *Reflectance Spectroscopy*; Interscience: New York, 1966, Chapter 3.

18. West, A. R. Solid State Chemistry and Its Applications; Wiley, New York, 1984, p. 51.

19. Lakowicz, J. R.; Gryczynski, I. Frequency-Domain Fluorescence Spectroscopy. In *Topics in Fluorescence Spectroscopy*; *Vol. 1. Techniques*; Lakowicz, J. R. Ed.; Plenum: New York, 1991, pp.293-336.

20. Sullivan, R. M.; Martin, J. D. "Understanding the Photoluminescence of Copper Aluminum Halide Phosphors." in *Luminescent Materials*, Ed.s, McKittrick, J.; Di Bartolo, B.; Mishra, K. *Proc. Mat. Res. Soc*., **1999**, *560*, 39-44.

21. Sing, K.S.W. Charachterization of Adsorbents. In *Adsorption, science and technology*; Rodrigues A. E.; LeVan M. D., Eds.; Kluwer Academic Publishers, Boston, 1989; pp.3-14.

22. (a) Liu, H.; Cirolo, M. F.; Grey, C. P.; Hanson, J.; Martin, J. D.; Sullivan, R. M. *BNL NSLS Activity Report*, **1997**, B-72. (b) Sullivan, R. M.; Martin, J. D.; Liu, H.; Grey, C. P.; Hanson, J. *BNL NSLS Activity Report*, **1998**, in press *www.nsls.bnl.gov/Pubs/ActivR/AR-98/MA1218.pdf*.

23. Monier, J-C.; Kern, R. *C. R. Hebd. Seances Acad. Sci.* **1955**, 241, 69.

24. Hildebrandkt, K.; Jones, P. G.; Schwarzmann, E.; Sheldrick, G. M. *Z. Naturforsch. B: Anorg. Chem. Org. Chem.* **1982**, 37, 1129.

25. Atom coordinates were taken from the single crystal structures. Default atomic parameters were used as found in the CAESAR adaptation of the Extended Hückel programs. Whangbo, M-H. *CAESAR*; Department of Chemistry, North Carolina State University: Raleigh, NC, 1998.

26. Pankove, J. *Optical Processes in Semiconductors*; Dover: New York, 1971, Chapter 3.

27. (a) Garro, N.; Cantarero, A.; Cardona, M.; Ruf, T.; Göbel, A.; Lin, C.; Reimann, K.; Rübenacke, S.; Stuebe, M. *Sol. State Comm.* **1996**, 98, 27. (b) Ferhat, M.; Zaoui, A.; Certier, M.; Khelifa, B. *Phys. Lett. A* **1996**, 216, 187.

28. (a) Brasser, R.; Pitt, E.; Scharmann, A.; Zimmer, G. *Phys. Stat. Sol. B*. **1975**, 69, 359. (b) Hameka, H. F.; Vlam, C. C. *Physica*, **1953**, 19, 943.

29. McGlynn, S. P.; Azumi, T.; Kinoshita, M. *Molecular Spectroscopy of the Triplet State*; Prentice-Hall: Englewood Cliffs, NJ, 1969; Chapter 3.

30. Forster, L. S. in Concepts of Inorganic Photochemistry; Adamson, A. W.; Fleischauer, P. D. Ed.s; Wiley, New York, p. 28.

31. (a) Ruthkosky, M.; Kelly, A.; Zaros, M. C.; Meyer, G. J. *J. Am. Chem. Soc.* **1997**, 119, 12004. (b) Balzani, V.; Carassiti, V. *Photochemistry of Coordination Compounds*; Academic: New York, 1970; Chapter 6.

32. Martin, J. D. *U. S. Patent* 5,876,637, 1999.

33. Ko, M. C.; Meyer, G. J. Photoluminescence of Inorganic Semiconductors for Chemical Sensor Applications in *Optoelectronic Properties of Inorganic Compounds*; Roundhill, D. M.; Fackler, J. P. Jr., Eds.; Modern Inorganic Chemsitry Series; Plenum: New York 1999, 269.

34. Lehninger. A. L. *Biochemistry; Second Edition*; Worth; New York: 1975, p 146.

35. Campbell, J. L. E.; Johnson, K. E. *J. Am. Chem. Soc.* **1989**, 111, 525.

36. Nicholson, D. G.; Winter, P. K.; Fineberg, H. in *Inorganic syntheses; Vol. III* ; Audrieth, L. F. Ed.; McGraw Hill: New York, 1950, 30.

37. Kauffman, G. B.; Fang, L. in *Inorganic syntheses; Vol. XXII*; Holt, S. L. Jr., Ed.; McGraw Hill: New York, 1983, p. 101.

38. Blasse, G.; Grabmaier, B. C., *Luminescent Materials*; Springer-Verlag: Berlin, 1994, p. A4.